CAT
Computer Aided Turbulence

User's Guide

Version 0.0

Hartmut Borth[1] Edilbert Kirk
Valerio Lucarini

[1]hartmut.borth@uni-hamburg.de

Contents

Part I

Model Physics

Chapter 1

Evolution equations of incompressible 2D fluids

1.1 Classical non-rotating case

The dimensional evolution equations of incompressible homogeneous 2D-fluids on the plane (see e.g. Batchelor [1967] or Canuto et al. [1988]) in vorticity velocity form

$$\zeta_t + \mathbf{u} \cdot \nabla\zeta = F + D, \tag{1.1}$$

with $\mathbf{u} = (u, v)$ the vector of velocity fields in x and y-direction, F a forcing and D a dissipation term. From homogeneity and incompressibility of the fluid we get

$$\nabla\cdot\rho\mathbf{u} = \rho\nabla \cdot \mathbf{u} = 0, \tag{1.2}$$

with ρ the fluid density. Using this property we can introduce a volume (mass) stream function measuring the volume (mass) flux across an arbitrary line from the point (x_0, y_0) to a point (x, y) via the path integral

$$\psi(x, y) - \psi(x_0, y_0) = -\int_{(x_0,y_0)}^{(x,y)} \left[\begin{pmatrix} u \\ v \end{pmatrix} \cdot \begin{pmatrix} -dy \\ dx \end{pmatrix} \right]. \tag{1.3}$$

The minus sign in front of the integral just changes the direction of positive massflux across the line and is chosen to make the classical stream function of 2D fluids compatible to the stream function (see e.g. Danilov and Gurarie [2000]) typically used for 2D rotating fluids in geosciences. In terms of the stream function ψ the integrated mass flux $\mathcal{M}$ across a line joining the points (x_0, y_0) and (x, y) is given by

$$\mathcal{M}(x_0, y_0|x, y) = -\rho H_0 \left[\psi(x, y) - \psi(x_0, y_0)\right], \tag{1.4}$$

with H_0 the depth of the fluid. At the same time the stream function ψ is connected to the velocity field (u, v) and the (relative) vorticity $\zeta = v_x - u_y$ via

$$(u, v) = (-\psi_y, \psi_x) \text{ and } \zeta = \Delta\psi. \tag{1.5}$$

Using the stream function ψ, the evolution equation (1.1 can be also written in the form

$$\zeta_t + J(\psi, \zeta) = F + D. \tag{1.6}$$

Since the velocity field is divergence free (equation 1.2) we can further derive the equivalent equation in flux form

$$\zeta_t + \nabla \cdot (\mathbf{u}\zeta) = F + D. \tag{1.7}$$

Starting from the flux form one can after repeated application of the continuity equation (1.2) finally derive an equation where the Jacobian only depends on the velocity two fields (u, v)

$$\zeta_t + \partial_x \partial_y \left(v^2 - u^2\right) + \left(\partial_x^2 - \partial_y^2\right) uv = F + D. \tag{1.8}$$

This form allows in the pseudo-spectral method (see 3.4) to reduce the number of Fourier transforms per time-step from 3, i.e. (u, v, ζ) to 2, i.e. (u, v).

1.2 Quasi-two-dimensional rotating case

Starting from the shallow water equation on the β-plane one can derive (see e.g. Danilov and Gurarie [2000]) an equation describing a rotating barotropic quasi-two-dimensional fluid which is a generalization of the 2D-equation (1.1). For small Rossby numbers $\mathrm{Ro} = U/Lf$, with U a typical horizontal fluid velocity at the length scale L considered and f the local coriolis paramter we get the potential vorticity (PV) q in quasi-geostrophic (QG) approximation

$$q = \left(\nabla^2 - \alpha^2\right) \psi + f, \tag{1.9}$$

where we have the modification parameter $\alpha = 1/L_{\mathrm{R}}^2$ with the Rossby-Obukhov radius of deformation $L_{\mathrm{R}} = \sqrt{gH_0}/f$ and the stream function $\psi = gh/f$. Here g is the gravitational acceleration and $h(x, y)$ the deviation of the mean fluid depth H_0 of the original shallow water layer. As in the 2-dimensional case the stream function ψ (remind the different definition) is related to the velocity fields (u, v) as defined in equation (1.5). In an unforced non-dissipative fluid the QG PV is materially conserved

$$q_t + J(\psi, q) = 0. \tag{1.10}$$

Using the linear approximation of the coriolis parameter $f = f_0 + \beta y$ and introducing again forcing and dissipation we can write the evolution equation in the form

$$q_t + J(\psi, q) + \beta \psi_x = F + D, \tag{1.11}$$

with the vorticity q given by

$$q = \left(\nabla^2 - \alpha^2\right) \psi = \zeta - \alpha^2 \psi. \tag{1.12}$$

Further one can introduce a variable mean fluid depth $H(x, y)$, which in the simple case of a linear slope in y-direction leads to a topographic β-effect (see e.g. Heijst [1994]).

In the form (1.11) and (1.12) one can simulate incompressible 2D fluids and rotating quasi-2D fluids with the same set of equations using different parameters. In this more general frame the simplest case of a non-rotating 2D incompressible fluid is characterized by a vanishing ambient vorticity gradient, i.e. $\beta = 0$, and the limit of an infinite Rossby radius $L_{\mathrm{R}} \longrightarrow \infty$ or a vanishing modification parameter $\alpha \longrightarrow 0$.

One only have to keep in mind that the stream functions different in the two cases. In the non-rotating case ψ is defined by equation (1.4). In the rotating case we get

$$h(x, y) = \frac{f}{g}\, \psi(x, y), \tag{1.13}$$

so that ψ is proportional to pressure deviations, which is not the case in the non-rotating 2D case where the relation is more complex, see e.g. Johnston and Liu [2004].

Using the property of the Jacobian $J(f, f) = 0$ for all fields $f(x, y)$ on the fluid domain equation (1.11) is equivalent to

$$q_t + J(\psi, \zeta) + \beta\psi_x = F + D, \tag{1.14}$$

where the vorticity q is still defined by equation (1.12). From this from it directly follows that that the form of the 2D Jacobian in equations (1.7) and (1.8) can be also applied in the quasi-two-dimensional rotating case.

1.3 Non-adiabatic terms

1.3.1 Laplacian based Viscosity and friction

Internal viscosity and external friction of the fluid are described by the dissipation term D on the left hand side of the equation (1.11). A classical way - the default reference in our model - to describe this term is to use a linear operator wich is a superposition of powers of the Laplacian. The default dissipation in the fluid simulator is defined by

$$D\ q = -\left[\sigma\,(-1)^{p_\sigma}\,\Delta^{p_\sigma} + \lambda\,(-1)^{p_\lambda}\,\Delta^{p_\lambda}\right] q. \tag{1.15}$$

Introducing dissipation time and length-scales we can write the dissipation operator also in the form

$$D\ q = -\left[\frac{(-1)^{p_\sigma}}{t_\sigma}\left(\frac{L_\sigma}{2\pi}\right)^{2p_\sigma}\Delta^{p_\sigma} + \frac{(-1)^{p_\lambda}}{t_\lambda}\left(\frac{L_\lambda}{2\pi}\right)^{2p_\lambda}\Delta^{p_\lambda}\right] q. \tag{1.16}$$

Here L_σ and L_λ are the small and large-scale cut-off length scales. The corresponding small and large-scale "damping" time scales are given by t_σ and t_λ. The powers p_σ of small-scale viscosity are in the range of $p_\sigma \in [1, 2, 3, \ \dots\ ]$ and the powers p_λ of large-scale friction are in the range $p_\lambda \in [0, -1, -2, -3, \ \dots\ ]$. For $p_\sigma = 1$ and $p_\lambda = 0$ we speak of viscosity and linear drag (friction), for $p_\sigma > 1$ and $p_\lambda < 0$ of hyperviscosity and hypofriction (see also Danilov and Gurarie [2001]). From equation (1.15) it follows that the coefficients σ and λ can be written by

$$\sigma = \left(\frac{L_\sigma}{2\pi}\right)^{2p_\sigma}\ \frac{1}{t_\sigma} = \left(\frac{1}{k_\sigma}\right)^{2p_\sigma}\ \frac{1}{t_\sigma}\ \text{ and }\ \lambda = \left(\frac{L_\lambda}{2\pi}\right)^{2p_\lambda}\ \frac{1}{t_\lambda} = \left(\frac{1}{k_\lambda}\right)^{2p_\lambda}\ \frac{1}{t_\lambda}. \tag{1.17}$$

We have chosen the additional factor of 2π since finally the fluid domain is rescaled to multiples of 2π. Using this scaling the coefficients σ and λ are characterized respectively by the damping the time scales t_σ and t_λ as well as the cut-off wave numbers k_σ and k_λ.

Above dissipation operator is a special case of dissipation operators which are polynomials with positive and negative powers of the Laplacian

$$Dq = \sum_{n=1}^{n_{max}} D_n q, \text{ with } D_n q = -\left[\sigma_{n-1}\,(-1)^{n-1}\ \Delta^{n-1}\ + \lambda_n\,(-1)^{-n}\ \Delta^{-n}\right]\ q. \tag{1.18}$$

In Fourier space (see subsection 3.4) the dissipation operators of this class reduce to the multiplication with polynomials in positive and negative powers of the wave numbers. More general dissipation operators can be constructed directly in Fourier space (see subsection 3.6).

1.3.2 Forcing

The forcing term F in equations (1.1) and (1.11) describes forcings due to either external processes as a wind-stress or a moving plate or non-resolved internal processes as, e.g. baroclinic instability or diabatic heating. Both types of forcings can be described in physical or spectral

space. For a constant external forcing, e.g. a wind stress or drag of a moving plate (τ^u, τ^v) given in $[N/m^2]$ and acting in x and y direction at the surface of the fluid the forcing term is given by

$$F(x,y) = \frac{1}{\rho H_0}\left(\tau_x^v - \tau_y^u\right), \tag{1.19}$$

where in the rotating quasi-2D case the height deviations h of the fluid are neglected. The forcing can also be defined in spectral space, see subsection 3.7 below.

1.4 Geometry and boundary conditions

1.4.1 Doubly periodic boundary condition

The evolution equations have to be completed by boundary conditions. The default geometry of the fluid domain is a square with an edge of length $L_x = L_y = L$ and the default boundary conditions are doubly periodic, i.e. $(f(x,y) = f(x+L, y+L)$ for all functions f on the fluid domain.

1.4.2 Channel boundary condition

In x-direction (zonal direction) we have periodic boudary conditions, i.e. $f(x,y) = f(x+L,y)$. In y-direction (meridional direction) at $y = 0$ and $y = L$ we introduce walls with no-slip boundary conditions, i.e. the meridional velocity at the walls is zero $v(x,0) = v(x,L) = 0$.

1.4.3 Box boundary condition

In x-direction (zonal direction) we introduce walls with no-slip boundary conditions, i.e. the zonal velocity at the walls is zero $u(0,y) = u(L,y) = 0$. In y-direction (meridional direction) at $y = 0$ and $y = L$ we introduce walls with no-slip boundary conditions, i.e. the meridional velocity at the walls is zero $v(x,0) = v(x,L) = 0$.

Part II

Numerical Implementation

Chapter 2

Model history

The roots of CAT go back to the 2D-turbulence model developed by Annalisa Bracco, see e.g. Bracco and McWilliams [2010]. The original model was redesigned in order to CAT integrate into the Planet Simulator model platform (PlaSim) **?**. The CAT code was rewritten from scratch **?** and complemented by a new stand-alone fft-library. Through the integration into the PlaSim platform the user of CAT has at his disposal a graphical user interface and a full model development environment. It is also possible to run CAT as a stand-alone application.

Chapter 3

The pseudo-spectral method

The idea behind the pseudo-spectral method is first to transform the evolution equations to Fourier (spectral) space, i.e. in our example to use the eigenfunctions of the Laplacian as basis of the space of all solutions and to project the full equations onto this basis, see e.g. Canuto et al. [1988]. Second to calculate products of functions (non-linear terms) in the physical space and transform them back to Fourier space to reduce the number of multiplications necessary, which otherwise makes the spectral method computationally prohibitively expensive for problems with a large numbers of Fourier modes. This idea goes back to Kreiss and Oliger [1972]. More details on the pseudospectral method can be found, e.g. in Orszag [1972] and Fornberg [1987].

3.1 The discrete Fourier transform

Starting point for the set of basis functions are the Fourier modes $F(k_x, k_y \mid x, y)$ which are the eigenmodes of the Laplacian on the fluid domain considered (short notation $F(\mathbf{k} \mid \mathbf{x})$ with $\mathbf{k} = (k_x, k_y)$ and $\mathbf{x} = (x, y)$). We start with a doubly periodic fluid domain (default in CAT). In this case the eigenmodes of the Laplacian are given by

$$F(\mathbf{k} \mid \mathbf{x}) = \exp\left[i\left(k_x x + k_y y\right)\right] = \exp\left[ik_x x\right]\ \exp\left[ik_y y\right], \tag{3.1}$$

and satisfy the eigenvalue equation

$$\Delta\ F(\mathbf{k} \mid \mathbf{x}) = -\left(k_x^2 + k_y^2\right)\ F(\mathbf{k} \mid \mathbf{x}), \tag{3.2}$$

with $k_x = n\ 2\pi/X$ and $k_y = m\ 2\pi/Y$ for $n, m \in [0, \pm 1, \pm 2,\ \ldots\ ]$. As can be seen form equation (3.1) the eigenmodes of the Laplacian on the two-dimensional fluid domain $F(\mathbf{k} \mid \mathbf{x}) = F(k_x \mid x)\ F(k_y \mid y)$ can be separated into a product of the eigenmodes of the 1-dimensional Laplacian. For more general domains as circular discs, annuli or the surface of spheres as well as for more general boundary conditions, i.e. for fluid domains with walls one has to choose other systems of basis functions, see e.g. Canuto et al. [1988].

Taking $L_x = X/2\pi$ and $L_y = Y/2\pi$ in x and y-direction as horizontal length scales and introducing the non-dimensional variables $\bar{x} = x/L_x$, $\bar{y} = y/L_y$, $\bar{k}_x = k_x L_x$ and $\bar{k}_y = k_y L_y$ the non-dimensional eigenvalue equation

$$\left[\frac{\partial^2}{\partial \bar{x}^2} + \frac{\partial^2}{r^2 \partial \bar{y}^2}\right]\ F(\bar{\mathbf{k}} \mid \bar{\mathbf{x}}) = -\left(\bar{k}_x^2 + \frac{\bar{k}_y^2}{r^2}\right) F(\bar{\mathbf{k}} \mid \bar{\mathbf{x}}), \tag{3.3}$$

with the aspect ratio of the fluid domain $r = L_y/L_y = Y/X$, the wave number vector $\bar{\mathbf{k}} = (\bar{k}_x, \bar{k}_y)$, where $\bar{k}_x = \bar{k}_y = 0, \pm 1, \pm 2,\ \ldots$ and the coordinate vector $\bar{\mathbf{x}} = (\bar{x}, \bar{y})$, where $\bar{x}, \bar{y} \in [0\ \ 2\pi]$. Such an approach leads to a rescaled Laplacian and is appropriate in particular for physical problems with a strong horizontal anisotropy.

Introducing a single horizontal length scale as for example $L = L_x = X/2\pi$ instead we get the non-dimensional variables $\bar{x} = x/L$, $\bar{y} = y/L$, $\bar{k}_x = k_x L = n$ and $\bar{k}_y/r = k_y L/r = m/r$. The non-dimensional eigenvalue equation now reads

$$\left[\frac{\partial^2}{\partial \bar{x}^2} + \frac{\partial^2}{\partial \bar{y}^2}\right] \; F(\bar{\mathbf{k}} \mid \bar{\mathbf{x}}) = -\left(\bar{k}_x^2 + \frac{\bar{k}_y^2}{r^2}\right) F(\bar{\mathbf{k}} \mid \bar{\mathbf{x}}), \tag{3.4}$$

with the aspect ratio of the fluid domain r defined above, the wave number vector $\bar{\mathbf{k}} = (\bar{k}_x, \bar{k}_y/r)$, where $\bar{k}_x = \bar{k}_y = 0, \pm 1, \pm 2, \ \ldots$ and the coordinate vector $\bar{\mathbf{x}} = (\bar{x}, \bar{y})$, where $\bar{x} \in [0 \ 2\pi]$ and $\bar{y} \in [0 \ r2\pi]$. In CAT we use a single horizontal length scale keeping in mind that this choice is not optimal for problems with a strong horizontal anisotropy. In the special case of a square domain (default case in CAT) we have $r = 1$. From now on we use, if not otherwise stated, the non-dimensional form and omit overbars.

Using the Fourier modes $F(\mathbf{k} \mid \mathbf{x})$ we can expand all fields $g(x, y, t)$ on the fluid domain into a Fourier series

$$g(x, y, t) = \sum_{k_x=-\infty}^{\infty} \sum_{k_y=-\infty}^{\infty} \hat{g}(k_x, k_y, t) \; \exp\left[i\left(k_x x + \frac{k_y}{r} y\right)\right], \tag{3.5}$$

where $\hat{g}(k_x, k_y, t)$ are the Fourier coefficients of $g(x, y, t)$ which live on the space of wave numbers (k_x, k_y). Since $g(x, y, t)$ are real fields, the Fourier modes $\hat{g}(k_x, k_y, t)$ have the symmetry property that

$$\hat{g}(-k_x, -k_y, t) = \hat{g}^*(k_x, k_y, t), \tag{3.6}$$

where g^* is the complex conjugate of g. The Fourier coefficients $\hat{g}(k_x, k_y, t)$ are obtained by the integral

$$\hat{g}(k_x, k_y, t) = \frac{1}{r}\frac{1}{4\pi^2} \int_0^{2\pi} \int_0^{r2\pi} \exp\left[-i\left(k_x x + \frac{k_y}{r} y\right)\right] \; g(x, y, t) \; dxdy. \tag{3.7}$$

This continous finite Fourier integral is derived from the dimensional integral

$$\hat{g}(k_x, k_y, t) = \frac{1}{XY} \int_0^X \int_0^Y \exp\left[-i\left(k_x x + k_y y\right)\right] \; g(x, y, t) \; dxdy, \tag{3.8}$$

where x,y,k_x and k_y are the dimensional variables.

To use the Fourier transform in numerical schemes to solve the evolution equation of fluids we have to approximate the continous finite Fourier integral (3.7) and the infinite Fourier series (3.5).

We start by discretizing the physical space into N grid points in x-direction and M grid points in y-direction. On the discretized grid of the physical space the continuous finite Fourier integral (3.7) reduces to the double sum

$$\hat{g}(k_x, k_y, t) = \frac{1}{NM} \sum_{n=0}^{N-1} \sum_{m=0}^{M-1} \exp\left[-i\left(k_x x_n + \frac{k_y}{r} y_m\right)\right] g(x_n, y_m, t), \tag{3.9}$$

where we use the approximations $dx = \Delta x = 2\pi/N$, $dy = \Delta y = r2\pi/M$, $x_n = n \ \Delta x$ and $y_m = m \ \Delta y$ with $n \in [0, 1, \ \ldots \ , N-1]$ and $m \in [0, 1, \ \ldots \ M-1]$. The aspect ratio of the grid cell is given by $\Delta x/\Delta y = M/N \ 1/r$. For $r = M/N$ the grid cells are squares (default in CAT $M = N$ and $r = 1$).

Next we truncate the infinite Fourier series (3.5) at wave numbers such that all modes with a higher spatial frequency (wave mumber) than the grid in physical space are omitted otherwise we would have an oversampling. The result is the finite sum

$$g(x_n, y_m, t) = \sum_{k_x=-\frac{N}{2}+1}^{\frac{N}{2}} \sum_{k_y=-\frac{M}{2}+1}^{\frac{M}{2}} \exp\left[i\left(k_x x_n + \frac{k_y}{r} y_m\right)\right] \; \hat{g}(k_x, k_y, t). \tag{3.10}$$

On the discretized grid in the physical space the modes with wave numbers $(k_x, k_y) = (-N/2, -M/2)$ and $(k_x, k_y) = (N/2, M/2)$ are identical. We omitted the mode $(k_x, k_y) = (-N/2, -M/2)$.

Using the definitions of $x_n = 2\pi\ n/N$ and $y_m = r2\pi\ m/M$ we can write equation (3.9) in discretized form as

$$\hat{g}(k_x, k_y, t) = \frac{1}{NM} \sum_{n=0}^{N-1} \sum_{m=0}^{M-1} \exp\left[-i2\pi\left(\frac{k_x n}{N} + \frac{k_y m}{M}\right)\right]\ g(x_n, y_m, t) \tag{3.11}$$

and equation (3.10) as

$$g(x_n, y_m, t) = \sum_{k_x=-\frac{N}{2}+1}^{\frac{N}{2}} \sum_{k_y=-\frac{M}{2}+1}^{\frac{M}{2}} \exp\left[i2\pi\left(\frac{k_x n}{N} + \frac{k_y m}{M}\right)\right] \hat{g}(k_x, k_y, t). \tag{3.12}$$

By a shift of the wave numbers k_x and k_y corresponding to a rotation in the complex plane the double sum (3.12) can be written equivalently in the form

$$g(x_n, y_m, t) = \sum_{k_x=0}^{N-1} \sum_{k_y=0}^{M-1} \exp\left[i2\pi\left(\frac{k_x n}{N} + \frac{k_y m}{M}\right)\right] \hat{g}(k_x, k_y, t). \tag{3.13}$$

Relation (3.11) defines the discrete 2-D forward Fourier transform $\mathcal{F}_{NM}$ and relation (3.13) the discrete 2-D inverse Fourier transform $\mathcal{F}_{MN}^{-1}$ respectively. One can decompose the 2-D transformations $\mathcal{F}_{NM}$ and $\mathcal{F}_{MN}^{-1}$ into two consecutive 1-D Fourier transformations $\mathcal{F}_N$, $\mathcal{F}_M$ and $\mathcal{F}_M^{-1}$, $\mathcal{F}_N^{-1}$.

The forward Fourier transform can be decomposed as follows

$$\hat{g}(k_x, k_y, t) = \frac{1}{N} \sum_{n=0}^{N-1} \exp\left(-i2\pi \frac{k_x n}{N}\right) \left[\frac{1}{M} \sum_{m=0}^{M-1} \exp\left(-i2\pi \frac{k_y m}{M}\right) g(x_n, y_m, t)\right] \tag{3.14}$$

or using operators $\hat{g} = \mathcal{F}_{NM}\ g = \mathcal{F}_N \mathcal{F}_M g$, where the operators $\mathcal{F}_N$ and $\mathcal{F}_M$ have the matrix representation

$$\mathcal{F}_N = \frac{1}{N}\ \left(exp\left[-i2\pi \frac{k_x n}{N}\right]\right)_{k_x, n \in [0, N-1]} \quad \text{and} \quad \mathcal{F}_M = \frac{1}{M}\ \left(exp\left[-i2\pi \frac{k_y m}{M}\right]\right)_{k_y, m \in [0, M-1]} \tag{3.15}$$

For the inverse Fourier transform we get the decomposition

$$g(x_n, y_m, t) = \sum_{k_y=0}^{M-1} \exp\left(i2\pi \frac{k_y m}{M}\right) \left[\sum_{k_x=0}^{N-1} \exp\left(i2\pi \frac{k_x n}{N}\right) \hat{g}(k_x, k_y, t)\right], \tag{3.16}$$

which using operators can be written as $g = \mathcal{F}_{MN}^{-1} = \mathcal{F}_M^{-1} \mathcal{F}_N^{-1} \hat{g}$, where the operators $\mathcal{F}_N^{-1}$ and $\mathcal{F}_M^{-1}$ have the matrix representation

$$\mathcal{F}_N^{-1} = \left(exp\left[i2\pi \frac{k_x n}{N}\right]\right)_{n, k_x \in [0, N-1]} \quad \text{and} \quad \mathcal{F}_M^{-1} = \left(exp\left[i2\pi \frac{k_y m}{M}\right]\right)_{m, k_y \in [0, M-1]}. \tag{3.17}$$

Using as basic unit the exponent $\omega = \exp[-i2\pi/N]$ we can represent the one-dimensional discrete forward Fourier transform $\mathcal{F}_N$ for a vector of length N as

$$\mathcal{F}_N = \frac{1}{N} \begin{pmatrix} 1 & 1 & 1 & \dots & 1 \\ 1 & \omega & \omega^2 & \dots & \omega^{N-1} \\ . & . & . & & . \\ . & . & . & & . \\ . & . & . & & . \\ 1 & \omega^{N-1} & \omega^{2(N-1)} & \dots & \omega^{(N-1)^2} \end{pmatrix}. \tag{3.18}$$

The representation of the Fourier matrices for small N are the building blocks of the fast Fourier transform introduced in section (3.2). For $N = 2$, $N = 3$ and $N = 4$ we get

$$\mathcal{F}_2 = \frac{1}{2}\begin{pmatrix} 1 & 1 \\ 1 & -1 \end{pmatrix}, \quad \mathcal{F}_3 = \frac{1}{3}\begin{pmatrix} 1 & 1 & 1 \\ 1 & \omega & \bar{\omega} \\ 1 & \bar{\omega} & \omega \end{pmatrix} \quad \text{and} \quad \mathcal{F}_4 = \frac{1}{4}\begin{pmatrix} 1 & 1 & 1 & 1 \\ 1 & -i & -1 & i \\ 1 & -1 & 1 & -1 \\ 1 & i & -1 & -i \end{pmatrix}, \tag{3.19}$$

with $\omega = -\exp(i\pi/3) = -(\cos(\pi/3) + i\ \sin(\pi/3))$. For $N = 8$ the representation reads

$$\mathcal{F}_8 = \frac{1}{8}\begin{pmatrix} 1 & 1 & 1 & 1 & 1 & 1 & 1 & 1 \\ 1 & \omega & -i & -i\omega & -1 & -\omega & i & i\omega \\ 1 & -i & -1 & i & 1 & -i & -1 & i \\ 1 & -i\omega & i & \omega & -1 & i\omega & -i & -\omega \\ 1 & -1 & 1 & -1 & 1 & -1 & 1 & -1 \\ 1 & -\omega & -i & i\omega & -1 & \omega & i & -i\omega \\ 1 & i & -1 & -i & 1 & i & -1 & -i \\ 1 & i\omega & i & -\omega & -1 & -i\omega & -i & \omega \end{pmatrix}, \tag{3.20}$$

with $\omega = \exp(-i\pi/4) = \sqrt{0.5}\ (1 - i) = \sqrt{2}\ (1 - i)/2$. The inverse Fourier transform $\mathcal{F}_N^{-1}$ is given by

$$\mathcal{F}_N^{-1} = \begin{pmatrix} 1 & 1 & 1 & \dots & 1 \\ 1 & \omega & \omega^2 & \dots & \omega^{N-1} \\ . & . & . & & . \\ . & . & . & & . \\ . & . & . & & . \\ 1 & \omega^{N-1} & \omega^{2(N-1)} & \dots & \omega^{(N-1)^2} \end{pmatrix}, \tag{3.21}$$

with $\omega = exp\,[i2\pi/N]$. The matrix representation (3.21) of the inverse FFT is related to the matrix representation (3.18) of the forward FFT by omission of the multiplication factor $1/N$ and the the replacement of ω by its complex conjugate $\bar{\omega}$. Using this rule it is straightforward to derive the matrix representations of the elementary inverse FFT operators $\mathcal{F}_2^{-1}$, $\mathcal{F}_3^{-1}$, $\mathcal{F}_4^{-1}$ and $\mathcal{F}_8^{-1}$.

Making full use of the information hidden in the structure of the Fourier matrices (forward and inverse) one can reduce the number of multiplications needed to carry out the Fourier transform from order $O(N^2)$ to order $O(N \log N)$, which makes a big difference for large N, see section 3.2.

3.2 Fast Fourier Transform

Keeping the matrix representation the decompostion of the discrete Fourier operator in order to reduce the number of multiplication can down in the case of a factor 2 decomposition in the following way. Rearranging the rows of a Fourier matrix $\mathcal{F}_N$ by collecting even and odd rows (assuming even N) we can express $\mathcal{F}_N$ in terms of $\mathcal{F}_{N/2}$ and get

$$\mathcal{F}_N\ \vec{g}_N = \begin{pmatrix} I_{N/2} & D_{N/2} \\ I_{N/2} & -D_{N/2} \end{pmatrix} \begin{pmatrix} \mathcal{F}_{N/2} & 0 \\ 0 & \mathcal{F}_{N/2} \end{pmatrix} \begin{pmatrix} \vec{g}^{\,1}_{N/2} \\ \vec{g}^{\,2}_{N/2} \end{pmatrix}, \tag{3.22}$$

where $\vec{g}^{\,1}_{N/2}$ and $\vec{g}^{\,2}_{N/2}$ are the odd and even components of the vector $\vec{g}_N$. Moreover $\mathcal{F}_{N/2}$ is the Fourier transform of size $N/2$, $I_{N/2} = diag_{N/2}(1, 1, \ \dots\ , 1)$ the identity matrix of size $N/2$

and $D_{N/2}$ the diagonal matrix $D_{N/2} = diag_{N/2}(1, \omega_N, \ \ldots \ , \omega_N^{N/2-1})$, with $\omega_N = \exp(-i2\pi/N)$. Transforming expression (3.22) further we can write

$$\mathcal{F}_N \ \vec{g}_N = \begin{pmatrix} I_{N/2} & I_{N/2} \\ I_{N/2} & -I_{N/2} \end{pmatrix} \begin{pmatrix} I_{N/2} & 0 \\ 0 & D_{N/2} \end{pmatrix} \begin{pmatrix} \mathcal{F}_{N/2} & 0 \\ 0 & \mathcal{F}_{N/2} \end{pmatrix} \ P_{2,N} \ \vec{g}_N \tag{3.23}$$

where $P_{2,N}$ is a permutation matrix reordering the vector components into 2 blocks (even and odd). Since the Fourier operators $\mathcal{F}_N$ are symmetric we can write the factor 2 decomposition also in the form

$$\mathcal{F}_N \ \vec{g}_N = \left[\mathcal{F}_2 \otimes I_{N/2}\right] \ \mathcal{D}_2 \ \left[I_2 \otimes \mathcal{F}_{N/2}\right] \ P_{2,N} \ \vec{g}_N, \tag{3.24}$$

where the direct matrix products $\left[\mathcal{F}_2 \otimes I_{N/2}\right]$ and $\left[I_2 \otimes \mathcal{F}_{N/2}\right]$ are defined as the following block matrices

$$\left[\mathcal{F}_2 \otimes I_{N/2}\right] = \begin{pmatrix} I_{N/2} & I_{N/2} \\ I_{N/2} & -I_{N/2} \end{pmatrix} \quad \text{and} \quad \left[I_2 \otimes \mathcal{F}_{N/2}\right] = \begin{pmatrix} \mathcal{F}_{N/2} & 0 \\ 0 & \mathcal{F}_{N/2} \end{pmatrix}. \tag{3.25}$$

The diagonal matrix $\mathcal{D}_2$ is given by $diag_2(I_{N/2}, D_{N/2})$. Using this decomposition we can reduce the order of the Fourier operator by two. Taking the Fourier operator $\mathcal{F}_4$ as first example we get

$$\mathcal{F}_4 \ \vec{g}_4 = \begin{pmatrix} 1 & 0 & 1 & 0 \\ 0 & 1 & 0 & 1 \\ 1 & 0 & -1 & 0 \\ 0 & 1 & 0 & -1 \end{pmatrix} \begin{pmatrix} 1 & 0 & 0 & 0 \\ 0 & 1 & 0 & 0 \\ 0 & 0 & 1 & 0 \\ 0 & 0 & 0 & -i \end{pmatrix} \begin{pmatrix} 1 & 1 & 0 & 0 \\ 1 & -1 & 0 & 0 \\ 0 & 0 & 1 & 1 \\ 0 & 0 & 1 & -1 \end{pmatrix} \begin{pmatrix} 1 & 0 & 0 & 0 \\ 0 & 0 & 1 & 0 \\ 0 & 1 & 0 & 0 \\ 0 & 0 & 0 & 1 \end{pmatrix} \ \vec{g}_4 \tag{3.26}$$

As we see the Fourier operator is decomposed into sparse matrices of a very simple form. For matrix entries with a 0 the multiplication and summation can be skipped. For entries with 1, -1, i and $-i$ multiplication can be skipped. Only signs have to be changed and if needed real parts have to be shifted to imaginary parts and vice versa. It is also possible to reduce the order of Fourier operators by a factor of 4. In this case the decomposition reads

$$\mathcal{F}_N \ \vec{g}_N = \left[\mathcal{F}_4 \otimes I_{N/4}\right] \ \mathcal{D}_4 \ \left[I_4 \otimes \mathcal{F}_{N/4}\right] P_{4,N} \ \vec{g}_N, \tag{3.27}$$

where

$$\left[\mathcal{F}_4 \otimes I_{N/4}\right] = \begin{pmatrix} I_{N/4} & I_{N/4} & I_{N/4} & I_{N/4} \\ I_{N/4} & -iI_{N/4} & -I_{N/4} & iI_{N/4} \\ I_{N/4} & -I_{N/4} & I_{N/4} & -I_{N/4} \\ I_{N/4} & iI_{N/4} & -I_{N/4} & -iI_{N/4} \end{pmatrix} \tag{3.28}$$

(3.29)

$$\left[I_4 \otimes \mathcal{F}_{N/4}\right] = \begin{pmatrix} \mathcal{F}_{N/4} & 0 & 0 & 0 \\ 0 & \mathcal{F}_{N/4} & 0 & 0 \\ 0 & 0 & \mathcal{F}_{N/4} & 0 \\ 0 & 0 & 0 & \mathcal{F}_{N/4} \end{pmatrix} \quad \text{and} \tag{3.30}$$

(3.31)

$$\mathcal{D}_4 = diag_4\left(I_{N/4}, D_{N/4}, D_{N/4}^2, D_{N/4}^3\right). \tag{3.32}$$

The permutation matrix $P_{4,N}$ maps the input vector $\vec{g}_N$ to $\left[\ \vec{g}^{\,1}_{N/4}, \vec{g}^{\,2}_{N/4}, \vec{g}^{\,3}_{N/4}, \vec{g}^{\,4}_{N/4}\ \right]$, a 4-component vector, with the $k{-}th$ components $\vec{g}^{\,k}_{N/4} = [\ k, k+4, k+8, \ldots, k+(N/4-1)\ 4\ ]$. Taking $N = 8$ as example and writing $P_{4,8}\ \vec{g}_8$ as a 4-component vector we get

$$\mathcal{F}_8 \ \vec{g}_8 = \frac{1}{4} \begin{pmatrix} I_2 & I_2 & I_2 & I_2 \\ I_2 & -iI_2 & -I_2 & iI_2 \\ I_2 & -I_2 & I_2 & -I_2 \\ I_2 & iI_2 & -I_2 & -iI_2 \end{pmatrix} \begin{pmatrix} I_2 & 0 & 0 & 0 \\ 0 & D_2 & 0 & 0 \\ 0 & 0 & D_2^2 & 0 \\ 0 & 0 & 0 & D_2^3 \end{pmatrix} \begin{pmatrix} \mathcal{F}_2 & 0 & 0 & 0 \\ 0 & \mathcal{F}_2 & 0 & 0 \\ 0 & 0 & \mathcal{F}_2 & 0 \\ 0 & 0 & 0 & \mathcal{F}_2 \end{pmatrix} \begin{pmatrix} \vec{g}^{\,1}_2 \\ \vec{g}^{\,2}_2 \\ \vec{g}^{\,3}_2 \\ \vec{g}^{\,4}_2 \end{pmatrix}, \tag{3.33}$$

with

$$D_2 = \begin{pmatrix} 1 & 0 \\ 0 & \omega \end{pmatrix}, \ \vec{g}_2^{\,k} = \begin{pmatrix} g_k \\ g_{k+4} \end{pmatrix} \ \text{ and } \ \omega = \sqrt{2}\,\frac{1-i}{2}. \tag{3.34}$$

Finally the FFT-scheme of CAT includes a factor 8 decomposition

$$\mathcal{F}_N\ \vec{g}_N = \left[\mathcal{F}_8 \otimes I_{N/8}\right]\ \mathcal{D}_8\ \left[I_8 \otimes \mathcal{F}_{N/8}\right] P_{8,N}\ \vec{g}_N, \tag{3.35}$$

with

$$\mathcal{D}_8 = diag_8\left(I_{N/8}, D_{N/8}, D_{N/8}^2, D_{N/8}^3 D_{N/8}^4, D_{N/8}^5, D_{N/8}^6, D_{N/8}^7\right). \tag{3.36}$$

Using the property that the fourier transform is a symmetric operator $\mathcal{F}_N^T = \mathcal{F}_N$ the above factorizations can also be written equivalently in different forms. For the factor 2, 4 and 8 decompositions we get

$$\mathcal{F}_N\ \vec{g}_N = P_{2,N}^T \left[I_2 \otimes \mathcal{F}_{N/2}\right] \mathcal{D}_2\ \left[\mathcal{F}_2 \otimes I_{N/2}\right]\ \vec{g}_N, \tag{3.37}$$

$$\mathcal{F}_N\ \vec{g}_N = P_{4,N}^T \left[I_4 \otimes \mathcal{F}_{N/4}\right] \mathcal{D}_4\ \left[\mathcal{F}_4 \otimes I_{N/4}\right]\ \vec{g}_N \quad \text{and} \tag{3.38}$$

$$\mathcal{F}_N\ \vec{g}_N = P_{8,N}^T \left[I_8 \otimes \mathcal{F}_{N/8}\right] \mathcal{D}_8\ \left[\mathcal{F}_8 \otimes I_{N/8}\right]\ \vec{g}_N. \tag{3.39}$$

The numerical implementation decomposes the original FFT operator $\mathcal{F}_N$ of order N recursively to a product of operators which only contain elmentary FFT operators $\mathcal{F}_{N_k}$ where the orders N_k are small prime numbers. In CAT the orders of the elementary operators used in the decomposition are $N_k = 2, 4, 8$. The inverse FFT can be decomposed in the same way as the forward FFT

$$\mathcal{F}_N^{-1}\ \vec{g}_N = \left[\mathcal{F}_2^{-1} \otimes I_{N/2}\right] \mathcal{D}_2^{-1}\ \left[I_2 \otimes \mathcal{F}_{N/2}^{-1}\right]\ P_{2,N}\vec{g}_N, \tag{3.40}$$

$$\mathcal{F}_N^{-1}\ \vec{g}_N = \left[\mathcal{F}_4^{-1} \otimes I_{N/4}\right] \mathcal{D}_4^{-1}\ \left[I_4 \otimes \mathcal{F}_{N/4}^{-1}\right] P_{4,N}\vec{g}_N \quad \text{and} \tag{3.41}$$

$$\mathcal{F}_N^{-1}\ \vec{g}_N = \left[\mathcal{F}_8^{-1} \otimes I_{N/8}\right] \mathcal{D}_8^{-1}\ \left[I_8 \otimes \mathcal{F}_{N/8}^{-1}\right]\ P_{8,N}\vec{g}_N. \tag{3.42}$$

Moreover we can again use the symmetry of the inverse FFT $\mathcal{F}_N^{-1} = \mathcal{F}_N^{-1\ T}$ to get the equivalent decomposition

$$\mathcal{F}_N^{-1}\ \vec{g}_N = P_{2,N}^T \left[I_2 \otimes \mathcal{F}_{N/2}^{-1}\right] \mathcal{D}_2^{-1}\ \left[\mathcal{F}_2^{-1} \otimes I_{N/2}\right]\ \vec{g}_N, \tag{3.43}$$

$$\mathcal{F}_N^{-1}\ \vec{g}_N = P_{4,N}^T \left[I_4 \otimes \mathcal{F}_{N/4}^{-1}\right] \mathcal{D}_4^{-1}\ \left[\mathcal{F}_4^{-1} \otimes I_{N/4}\right]\ \vec{g}_N \quad \text{and} \tag{3.44}$$

$$\mathcal{F}_N^{-1}\ \vec{g}_N = P_{8,N}^T \left[I_8 \otimes \mathcal{F}_{N/8}^{-1}\right] \mathcal{D}_8^{-1}\ \left[\mathcal{F}_8^{-1} \otimes I_{N/8}\right]\ \vec{g}_N. \tag{3.45}$$

Due to the sparse matrices with the special direct product structure it is much more efficient to implement the FFT operator decompositions given in euqations (3.22) to (3.35) or (3.37) to (3.39) not as matrix operators but directly as permuations of memory addresses and hard-coded arithmetic operations.

Text FFT Edilbert?

3.3 The grid representation in CAT

In physical space all fields $g(x, y)$ are real and are represented on a regular grid. Figure 3.1 shows the grid for a horizontal resolution of $ngx = ngy = 16$. Grid point fields read or written by CAT are given in this format. The corresponding fields in spectral space are complex. Internally in CAT they are either represented as complex $c(k_x, k_y)$ or as real $f(k_x, k_y)$ fields. Plate (a) in figure 3.2 shows the wave number grid for the internal complex representation

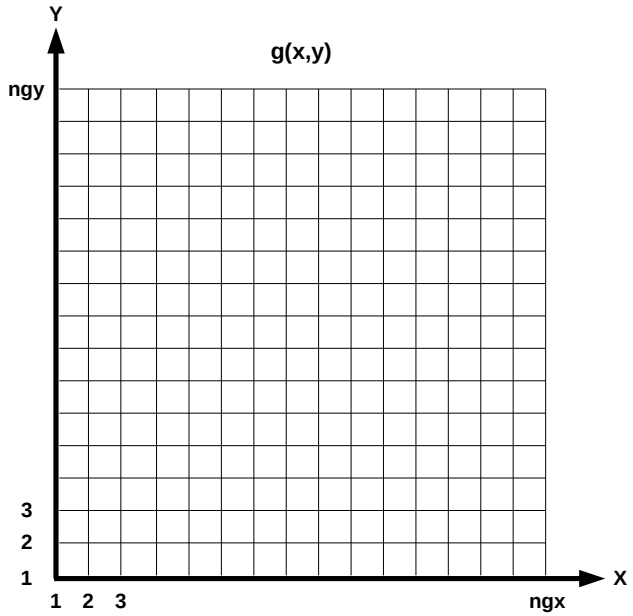

Figure 3.1: In physical space functions $g(x, y)$ are represented on a regular grid with ngx grid points in x-direction and ngy grid points in y-direction. At present in CAT only the default $ngx = ngy$ is implemented.

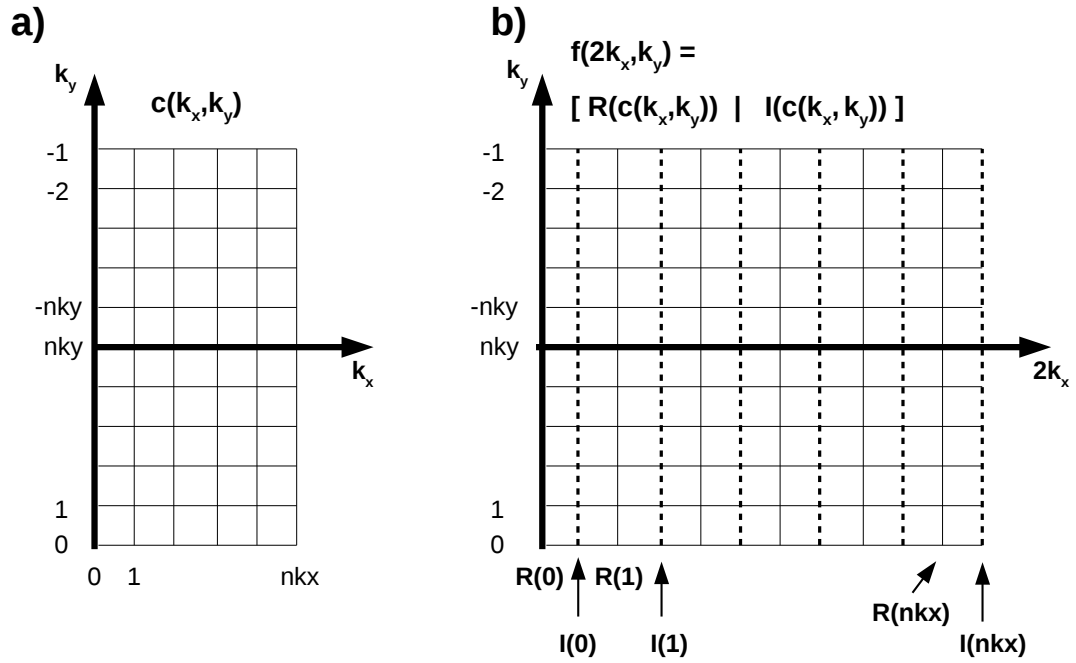

Figure 3.2: Functions in spectral space are represented either as complex fields c (plate a) or as real fields f containing in the first spectral coordinate k_x the real and imaginary parts of c in an alternating series (plate b).

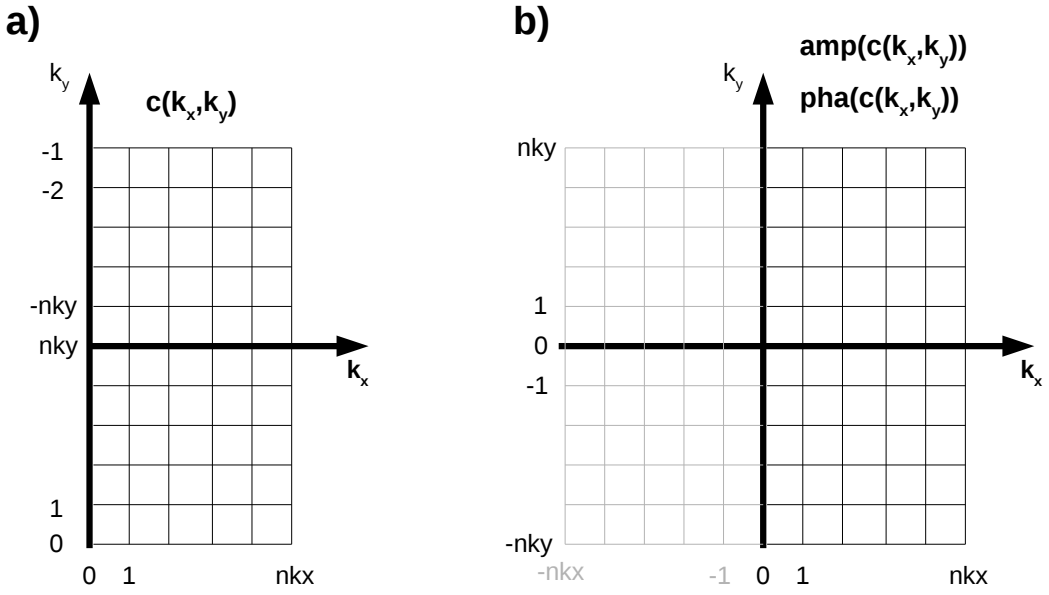

Figure 3.3: Internally (plate a) complex spectral fields c are defined on the non-centered wave number grid given by (3.46). To visualize complex spectral fields (plate b) amplitudes $amp(c)$ and phases $pha(c)$ are sent to the graphical user interface (GUI) on the centered wave-number grid given by (3.48).

$c(k_x, k_y)$ of spectral fields. Due to the symmetry properties 3.6 it is sufficient to represent the spectral fields c only on half of the wave number space, i.e. only for the wave numbers

$$(k_x,\ k_y) \in \{\ k_x \in [\ 0, 1,\ \ldots\ nkx\ ]\ \text{ and }\ k_y \in [\ 0,\ \ldots\ , nky, -nky,\ \ldots\ , -1\ ]\}. \tag{3.46}$$

As described above we use the 2/3-truncation, so that the bounds nkx and nky are given by

$$nkx = ngx/3\ \text{ and }\ nky = ngy/3, \tag{3.47}$$

where the non-integer part of the division is omitted. In our example $ngx = 8$ from above $nkx = nky = 16$. The wave-numbers in y-direction are not centered around zero. Plate (b) of figure 3.2 shows the internal real representation $f(k_x, k_y)$ of spectral fields. In y-direction the spectral grid is the same for the complex c and the real representation f. In x-direction the number of coordinate points is doubled for the real representation. Even coordinates starting from 0 hold the real part $\mathcal{R}(c(k_x, k_y))$ and the odd coordinates starting from 1 the imaginary part $I(c(k_x, k_y))$ of the complex fields $c(k_x, k_y)$. This is the format CAT reads in or writes out spectral fields. Prescribing complex spectral fields $c(k_x, k_y)$ in CAT it is important to keep in mind that on the k_y-axis ($k_x = 0$) values are not arbitrary, otherwise unphysical complex fields are created in grid point (physical) space. First $c(0, 0)$ has to be real, they are the average of the field $g(x, y)$ in physical space. In the case of vorticity cq we get in the special case of a doubly periodic domain $cq(0, 0) = 0$. For the remaining values $(0, k_y)$ the symmetry properties 3.6 have to be satisfied, i.e. on the k_y-axis spectral fields must satisfy the condition $c(0, k_y) = c^*(0, -k_y)$. In the Graphical User Interface (GUI) spectral fields are visualized on a centerd wave-number

grid

$$(k_x,\ k_y) \in \{\ k_x \in [\ -nkx,\ \ldots\ , nkx\ ]\ \text{ and }\ k_y \in [\ -nky,\ \ldots\ , nky\ ]\ \}. \tag{3.48}$$

Visualized are the amplitudes $amp(c)$ and phases $pha(c)$ of the complex fields

$$amp(k_x, k_y) = \sqrt{\mathcal{R}^2(c) + I^2(c)}\ \text{ and }\ pha(k_x, k_y) = \tan^{-1}(\frac{I(c)}{\mathcal{R}(c)}). \tag{3.49}$$

By the symmetry properties 3.6 of spectral fields c the amplitudes $amp(c)$ are symmetric with respect to the k_y-axis and the phases $pha(c)$ are point symmetric with respect to the origin $(0, 0)$ of the grid of wave numbers. For visualization amplitudes amp and phases pha are thus represented on the left half space of centered wave numbers denoted by the solid bold black grid given in plate (b) of figure 3.3 including the k_y-axis.

Using the amplitudes $amp(k_x, k_y)$ and phases $pha(k_x, k_y)$ defined on the grid (3.46) one can represent a complex field $c(k_x, k_y)$ as follows

$$c(k_x, k_y) = amp(c(k_x, k_y))\ exp[\ i\ pha(c(k_x, k_y))]\,. \tag{3.50}$$

This representation is used to define forcing fields in spectral space.

3.4 Evolution equations in Fourier space

The basic advantage of the Fourier representation is that differential operators as ∂_x, ∂_y, $\partial_x\partial_y$, ∇, Δ are transformed to simple multiplication operators ik_x, ik_y/r, $-k_xk_y/r$,$(ik_x, ik_y/r)$, $-(k_x^2 + k_y^2/r^2)$ in spectral space with $i = \sqrt{-1}$. Differential equations in physical space are thus reduced to algebraic equations in spectral space.

In the Fourier space it is now straight forward to determine the stream function $\hat{\psi}(k_x, k_y, t)$ and the corresponding velocity fields $\hat{u}(k_x, k_y, t)$ and $\hat{v}(k_x, k_y, t)$ once the vorticity field $\hat{q}(k_x, k_y, t)$ is known. The vorticity equation (1.12) of the quasi-2D rotating case reduces to

$$-\left(k_x^2 + \frac{k_y^2}{r^2} + \alpha^2\right)\hat{\psi}(k_x, k_y, t) = \hat{q}(k_x, k_y, t), \tag{3.51}$$

which in the case for $\alpha \neq 0$ can always be solved for the stream function

$$\hat{\psi}(k_x, k_y, t) = -\frac{1}{k_x^2 + k_y^2/r^2 + \alpha^2}\ \hat{q}(k_x, k_y, t). \tag{3.52}$$

In the case $\alpha = 0$ equation (3.52) is still valid except for the zero mode. Here we set $\hat{\psi}(0, 0, t) = 0$, which is consistent with the definition (1.13) of the stream function and the double periodic boundary conditions. Further the velocity field is simply given by

$$\hat{u}(k_x, k_y, t) = -i\frac{k_y}{r}\ \hat{\psi}(k_x, k_y, t) = i\ \frac{k_y/r}{k_x^2 + k_y^2/r^2 + \alpha^2}\ \hat{q}(k_x, k_y, t) \tag{3.53}$$

and

$$\hat{v}(k_x, k_y, t) = ik_x\ \hat{\psi}(k_x, k_y, t) = -i\ \frac{k_x}{k_x^2 + k_y^2/r^2 + \alpha^2}\ \hat{q}(k_x, k_y, t). \tag{3.54}$$

In spectral space the evolution equations of the general quasi-2D rotating case can be separated into individual ordinary differential equations. For every wave number pair $\mathbf{k} = (k_x, k_y)$ we get

$$\frac{d}{dt}\ \hat{q}_\mathbf{k} = i\ \frac{k_x\beta}{k_x^2 + k_y^2/r^2 + \alpha^2}\ \hat{q}_\mathbf{k} - \hat{J}_\mathbf{k} + \hat{F}_\mathbf{k} + \hat{D}_\mathbf{k}. \tag{3.55}$$

For vanishing Jacobian, Forcing and Dissipation terms we get a linear equation

$$\frac{d}{dt}\ \hat{q}_{\mathbf{k}} = i\ \frac{k_x\beta}{k_x^2 + k_y^2/r^2 + \alpha^2}\ \hat{q}_{\mathbf{k}} \tag{3.56}$$

which can be solved exactly

$$\hat{q}_{\mathbf{k}}(t) = \exp\left[i\ \frac{k_x\beta}{k_x^2 + k_y^2/r^2 + \alpha^2}\ \Delta t\right]\ \hat{q}_{\mathbf{k}}(t_0), \tag{3.57}$$

with $\hat{q}_{\mathbf{k}}(t_0)$ the initial condition at time t_0 and the time interval $\Delta t = t - t_0$. The β-term induces a wave number dependend phase-shift. If one includes a linear dissipation term $\hat{D}_{\mathbf{k}}$ the evolution equation can still be solved exactly (see subsection 3.6). The Jacobian $\hat{J}_{\mathbf{k}}$, forcing $\hat{F}_{\mathbf{k}}$ and dissipation $\hat{D}_{\mathbf{k}}$ terms are described in detail below.

3.5 Jacobian

The non-linearity of the Jacobian makes it numerically too expensive to solve it exclusively in spectral space. The individual terms in the products of the Jacobian are first differentiated in spectral space and then transformed back to the physical space. There the terms are multiplied and the products are then transformed back to spectral space. Due to this back and forth transfomations the method is not purely spectral and is called pseudo-spectral method, see e.g. Kreiss and Oliger [1972] and Orszag [1972]. Due to the products the higher wave numbers have to be filtered out. In CAT trunction is used, see above.

We present three different forms of the Jacobian J in physical space, see equations (1.6), (1.7) and (1.8). Using the pseudo-spectral method for each form we get a different representation of the Jacobian $\hat{J}$ in spectral space.

For the Jacobian (1.6) of the first form

$$J(\psi,\zeta) = J(\psi,q) = \partial_x\psi\ \partial_y q - \partial_x q\ \partial_y\psi = \left[v\ \partial_y q + u\ \partial_x q\right], \tag{3.58}$$

one proceeds as follows. First the individual differential terms are determined in spectral space using the fourier transform of vorticity, and the spectral representation of the differential operators. We get

$$\mathcal{F}(\partial_x\psi) = ik_x\ \mathcal{F}(\psi) = \mathcal{F}(v) = -\ i\ \frac{k_x}{k_x^2 + k_y^2 + \alpha}\ \mathcal{F}(q),\quad \mathcal{F}(\partial_y q) = ik_y\ \mathcal{F}(q) \tag{3.59}$$

$$\mathcal{F}(\partial_y\psi) = ik_y\ \mathcal{F}(\psi) = -\mathcal{F}(u) = -\ i\ \frac{k_y}{k_x^2 + k_y^2 + \alpha}\ \mathcal{F}(q),\quad \mathcal{F}(\partial_x q) = ik_x\ \mathcal{F}(q). \tag{3.60}$$

Next all four terms defined by equations (3.59) and (3.60) are transformed to physical space. In physical space the Jacobian $J(\psi,\zeta)$ is then calculated following the definition (3.58) and finally transformed back to spectral space. The Jacobian in spectral space $\hat{J}$ is given by

$$\hat{J} = \mathcal{F}(v\partial_y q) - \mathcal{F}(u\partial_x q). \tag{3.61}$$

Combining all necessary steps we can write

$$\begin{aligned}\hat{J} &= \mathcal{F}\left(\mathcal{F}^{-1}\left(-\ i\frac{k_x}{k_x^2 + k_y^2 + \alpha}\ \hat{q}\right)\mathcal{F}^{-1}\left(ik_y\ \hat{q}\right)\right)\\ &- \mathcal{F}\left(\mathcal{F}^{-1}\left(\ i\frac{k_y}{k_x^2 + k_y^2 + \alpha}\ \hat{q}\right)\mathcal{F}^{-1}\left(ik_x\ \hat{q}\right)\right),\end{aligned} \tag{3.62}$$

where $\hat{q}$ is the vorticity in spectral space, the starting point for a new time step. As can be seen one needs 6 2-FFT operations to determine the Jacobian. The components of the Jacobian $\hat{J}_k$ are then used to determine the time evolution of the different wave number components of the vorticity $\hat{q}_{\mathbf{k}}$, see equation (3.55).

In the flux form of the evolution equation (1.7) the second form of the Jacobian arises

$$J(\psi, q) = \partial_x(u\ q) + \partial_x(v\ q). \tag{3.63}$$

Following again equations (3.59) and (3.60) we determine $\mathcal{F}(u)$ and $\mathcal{F}(v)$. Then $\mathcal{F}(u)$, $\mathcal{F}(v)$ and $\mathcal{F}(q)$ are transformed to the physical space,where the products uq and vq are formed. Finally the products are transformed back to spectral space where they are differentiated. The Jacobian $\hat{J}$ in spectral space is then given by

$$\hat{J} = ik_x\ \mathcal{F}(uq) + ik_y\ \mathcal{F}(vq). \tag{3.64}$$

Combining again all necessary steps we can write

$$\begin{aligned} \hat{J} &= ik_x\ \mathcal{F}\left(\mathcal{F}^{-1}\left(\ i\frac{k_y}{k_x^2+k_y^2+\alpha}\ \hat{q}\right)\mathcal{F}^{-1}\left(\hat{q}\right)\right) \\ &+ ik_y\ \mathcal{F}\left(\mathcal{F}^{-1}\left(\ -\ i\frac{k_x}{k_x^2+k_y^2+\alpha}\ \hat{q}\right)\mathcal{F}^{-1}\left(\hat{q}\right)\right). \end{aligned} \tag{3.65}$$

As we can see the Jacobian in spectral space $\hat{J}$ can now be determined by 5 FFT operations.

The third form of the Jacobian used in equation (1.8) is given by

$$J(\psi, q) = \partial_x\partial_y\left(v^2 - u^2\right) + \partial_x^2\partial_y^2 uv. \tag{3.66}$$

In this representation it is possible to reduce the number of FFT operations from 5 to 4. We first have to determine $\hat{u}$ and $\hat{v}$ following equations (3.59) and (3.59) and then to transform them to physical space where the products $v^2 - u^2$ and uv are formed. Finally we have to transform them back to spectral space where they are differentiated. The Jacobian in spectral space $\hat{J}$ is given by

$$\hat{J} = -k_x k_y\ \mathcal{F}(v^2 - u^2) + k_x^2 k_y^2 \mathcal{F}(uv) \tag{3.67}$$

or by combining all necessary steps

$$\begin{aligned} \hat{J} &= -\ k_x k_y\ \mathcal{F}\left(\left[\mathcal{F}^{-1}\left(\ -\ i\frac{k_x}{k_x^2+k_y^2+\alpha}\ \hat{q}\right)\right]^2 - \left[\mathcal{F}^{-1}\left(\ i\frac{k_y}{k_x^2+k_y^2+\alpha}\ \hat{q}\right)\right]^2\right) \\ &+ k_x^2 k_y^2\ \mathcal{F}\left(\mathcal{F}^{-1}\left(\ i\frac{k_y}{k_x^2+k_y^2+\alpha}\ \hat{q}\right)\mathcal{F}^{-1}\left(\ -\ i\frac{k_x}{k_x^2+k_y^2+\alpha}\ \hat{q}\right)\right). \end{aligned} \tag{3.68}$$

One can also use hybrid forms of the Jacobian which are a linear combination of the three forms given above.

3.6 Dissipation

In CAT the default parameterization of viscosity (internal dissipation) and friction (dissipation at the horizontal boundaries of the fluid) is based on positive and negative powers of the Laplacian (see equation 1.15). In spectral space the dissipation operator is given by the linear superposition

$$\hat{D}_{\mathbf{k}}\hat{q}_{\mathbf{k}} = -\left[\sigma\left(k_x^2+k_y^2\right)^{p_\sigma} + \lambda\left(k_x^2+k_y^2\right)^{p_\lambda}\right]\hat{q}_{\mathbf{k}}. \tag{3.69}$$

Using the definitions σ and λ of (1.17) we can write the dissipation operator (3.69) in the form

$$\hat{D}_{\mathbf{k}}\hat{q}_{\mathbf{k}} = -\left[\frac{1}{t_\sigma}\left(\frac{1}{k_\sigma}\right)^{2p_\sigma}\left(k_x^2+k_y^2\right)^{p_\sigma} + \frac{1}{t_\lambda}\left(\frac{1}{k_\lambda}\right)^{2p_\lambda}\left(k_x^2+k_y^2\right)^{p_\lambda}\right]\hat{q}_{\mathbf{k}}. \tag{3.70}$$

Mind that $p_\lambda \leq 0$. A dissipation term based on the superposition of powers of Laplacian is a multiplication operator in the spectral space. Introducing the radius $r_{\mathbf{k}} = \sqrt{k_x^2+k_y^2}$ in spectral space the dissipation operator can be written as

$$\hat{D}_{\mathbf{k}}\hat{q}_{\mathbf{k}} = -\left[\sigma\ r_{\mathbf{k}}^{2p_\sigma} + \lambda\ r_{\mathbf{k}}^{2p_\lambda}\right]\hat{q}_{\mathbf{k}}. \tag{3.71}$$

Using linear superpositions of different powers of the Laplacian as defined in (1.18) we get in Fourier space the more general dissipation operator

$$\hat{D}_{\mathbf{k}}\hat{q}_{\mathbf{k}} = \sum_{n=1}^{n_{max}} \hat{D}_{\mathbf{k},n}\hat{q}_{\mathbf{k}}, \quad \text{with} \quad \hat{D}_{\mathbf{k},n}\hat{q}_{\mathbf{k}} = -\left[\sigma_{n-1}\ r_{\mathbf{k}}^{2(n-1)} + \lambda_n\ r_{\mathbf{k}}^{-2n}\right]\hat{q}_{\mathbf{k}}. \tag{3.72}$$

Including the dissipation operator described above into the equation (3.56) we get for every wave number $\mathbf{k}$ the linear evolution equation

$$\frac{d}{dt}\ \hat{q}_{\mathbf{k}} = \left[i\ \frac{k_x\beta}{k_x^2+k_y^2/r^2+\alpha^2} - \sum_{n=1}^{n_{max}}\left[\sigma_{n-1}r_{\mathbf{k}}^{2(n-1)} + \lambda_n r_{\mathbf{k}}^{-2n}\right]\right]\ \hat{q}_{\mathbf{k}}, \tag{3.73}$$

which has the exact solution

$$\hat{q}_{\mathbf{k}}(t) = \exp\left[i\ \frac{k_x\beta}{k_x^2+k_y^2/r^2+\alpha^2}\ \Delta t\right]\ \exp\left[-\sum_{n=1}^{n_{max}}\left(\sigma_{n-1}r_{\mathbf{k}}^{2(n-1)} + \lambda_n r_{\mathbf{k}}^{-2n}\right)\Delta t\right]\ \hat{q}_{\mathbf{k}}(t_0), \tag{3.74}$$

with $\hat{q}_{\mathbf{k}}(t_0)$ the initial condition at time t_0 and the time interval $\Delta t = t - t_0$. As the solution (3.74) shows the dissipation operator introduces a wave-number dependent exponential damping without phase shift.

Considering the connection between convolutions and Fourier transforms $f * g = \hat{f}\hat{g}$ the dissipation operator can be seen as a special spectral filter. Using the filter approach one can introduce more general dissipation operators. Figure 3.4 shows a a simple cut-off filter given by

$$\hat{q}_{\mathbf{k}}(t) = \begin{cases} \hat{q}_{\mathbf{k}}(t) & \text{for } \mathbf{k} \text{ with } \quad r_{min} \leq |r_{\mathbf{k}}| \leq r_{max} \\ 0 & \text{otherwise.} \end{cases} \tag{3.75}$$

With higher order exponential functions one can create a smoothed cut-off filter.

3.7 Forcing

3.8 Time-stepping schemes

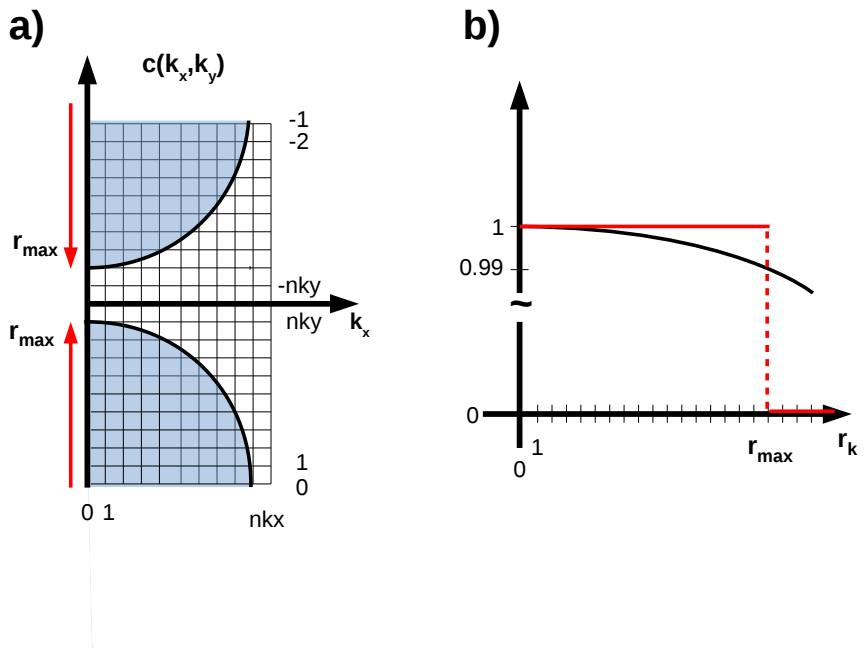

Figure 3.4: Cut-off (plate a) and gaussian filter (plate b) in spectral space.

Chapter 4

Predefined simulations, test cases and performance

In CAT different series of predefined simulations are implemented. They comprise simple idealized examples allowing the study of basic propeties of 2D and rotating balanced flows. Further simulations of previous studies are included allowing the reproduction reference cases.

4.1 Initial Value Problems in Physical Space

Initial value problems in physical space simulate the time evolution of vorticity (potential vorticity) distributions prescribed in physical space under the action of dissipation. The predefined simulations can be seen on the one hand as illustrative examples for teaching purposes and on the other hand as starting point for new and more general simulations.

4.1.1 Top Hat Jet: Option `sim = "jet01"`

4.1.2 Gaussian Jet: Option `sim = "jet02"`

4.1.3 Fourier Jet: Option `sim = "jet03"`

4.1.4 Circular Top Hat Jet: Option `sim = "jet04"`

4.1.5 Circular Gaussian Jet: Option `sim = "jet05"`

4.1.6 Circular Fourier Jet: Option `sim = "jet06"`

4.1.7 Elliptical Vortex Patches: Option `sim = "vor01"`

4.1.8 Elliptical Gaussian Vortices: Option `sim = "vor02"`

4.2 Initial Value Problems in Spectral Space

Initial value problems in spectral space simulate the time evolution of vorticity (potential vorticity) distributions prescribed in spectral space under the action of dissipation. This class of simulations contains as a special case the classical decaying turbulence experiments.

4.2.1 discs in Fourier Space: Option `sim = "dec01"`

4.2.2 Rings in Fourier Space: Option `sim = "dec01"`

4.3 Forced decaying flows

Part III

Using CAT

Chapter 5

Implementing CAT

Chapter 6

Running CAT

Chapter 7

Analysing CAT output

Chapter 8

Modifying CAT

Part IV

Appendix

Appendix A

Namelists and parameters

To set-up a CAT simulation different types of namelists are available. A CAT namelist cat_nl to control the numerics and physics of CAT simulations in general and a simulation namelist sim_nl which specifies a list of predefined simulations.

CAT control: cat_nl

We have subdivided the control parameters of CAT into a group of model numerics and model physics.

Model set-up

parameter	default	options, description and type
nx	64	grid points in x-direction (integer)
ny	64	grid points in y-direction (integer) [not active ny = nx]
nl	1	number of layers (integer) [not active]
nsteps	10000	number of time steps to be integrated (integer)
ngp	100	time steps between output of grid-point fields (integer)
nsp	100	time steps between output of spectral fields (integer)
ngui	1	1/0 graphical user interface on/off (integer)

Physics

parameter	default	options and description
jac_mthd	1	approximation method of Jacobian 0 : no Jacobian 1 : divergence form

Postprocessing

parameter	default	options and description
npost	0	1/0 additional postprocessing on/off

Predefined simulations: sim_nl

With activated predefined

Simulations

parameter	default	options and description

sim	`"dec01"`	class of predefined simulations (character array)
		`"dec01" : decaying turbulence`
		`"for01" : forced decaying turbulence`
		`"jet01" : top-hat jet`
		`"vor01" : gaussian elliptical vortex`

Appendix B

Moduls and basic model variables

Appendix C

Structure of code and flow scheme

Bibliography

G. K. Batchelor. An Introduction to Fluid Dynamics. Cambridge University Press, 615 pp, 1967.

A. Bracco and J. C. McWilliams. Reynolds-number dependency in homogeneous, stationary two-dimensional turbulence. *J.* Fluid Mech., 646:517–526, 2010.

C. Canuto, M.Y. Hussaini, A. Quarteroni, and T.A. Zhang. Spectral Methods in Fluid Dynamics. Spinger Series in Computational Physics. Spinger, Spinger-Verlag Berlin Heidelberg, 1988.

S. Danilov and D. Gurarie. Quasi-two-dimensional turbulence. Physics-Uspekhi, 43:863–900, 2000.

S. Danilov and D. Gurarie. Forced two-dimensional turbulence in spectral and physical space. *Phys.* Rev. E, 63:061208, 2001.

B. Fornberg. The pseudospectral method: Comparison with finite differences for the elastic wave equation. *Geophysics*, 52:483–501, 1987.

G.J.F. Van Heijst. Topography Effects on Vortices in a Rotating Fluid. *Meccanica*, 29:431–451, 1994.

H. Johnston and J.-G. Liu. Accurate, stable and efficient Navier-Stokes solvers based on explicit treatment of the pressure term. *J.* Comput. Phys., 199:221–259, 2004.

H.-O. Kreiss and J. Oliger. Comparison of accurate methods for the integration of hyperbolic equations. *Tellus*, 24:199–215, 1972.

S. Orszag. Comparison of pseudospectral and spectral approximation. *Stud.* Appl. Math., 51: 253–259, 1972.